

Lossless polarization attraction of telecom signals: application to all-optical OSNR enhancement

Matteo Barozzi^{1,*} and Armando Vannucci¹

¹*Dipartimento di Ingegneria dell'Informazione, Università degli Studi di Parma, viale delle Scienze 181/A, 43124 Parma, Italy*

*Corresponding author: matteo.barozzi82@gmail.com

Received July 24, 2014; accepted August 26, 2014;
posted September 10, 2014 (Doc. ID 217763); published October 16, 2014

We propose an all-optical fiber-based device that is able to accomplish polarization control and OSNR enhancement of an amplitude modulated optical signal at the same time. The proposed device is made of a nonlinear lossless polarizer (NLP), which performs polarization control, followed by an ideal polarizing filter, which removes the orthogonally polarized half of additive noise. The task of the NLP is to impose signal polarization aligned with the transparent eigenstate of the polarizing filter. In order to effectively control the polarization of an amplitude modulated signal in the presence of additive noise, we show how one of the two different NLP configurations (with counter- or co-propagating pump laser) is needed, as a function of the signal polarization coherence time. We demonstrate that an OSNR gain close to 3 dB can be achieved by using the proper NLP configuration. Finally, we show how the achievable OSNR gain can be estimated theoretically. © 2014 Optical Society of America

OCIS codes: (230.5440) Polarization-selective devices; (060.4370) Nonlinear optics, fibers; (060.2360) Fiber optics links and subsystems; (230.1150) All-optical devices; (230.4320) Nonlinear optical devices; (190.3270) Kerr effect.

<http://dx.doi.org/10.1364/JOSAB.31.002712>

1. INTRODUCTION

Controlling the state of polarization (SOP) of an optical signal is an open issue in optical transmission systems and optical signal processing and has been a subject of intense research ([1], and references therein). Among the different techniques that have been proposed, to control polarization (e.g., by exploiting Raman gain [2–8], Brillouin scattering [9], or photorefractive materials [10]), we shall concentrate here on lossless polarization attraction (LPA) [11,12]. LPA is a nonlinear two-channel phenomenon, based on the Kerr effect, occurring between the signal whose SOP has to be controlled and a fully polarized continuous wave (CW) pump beam. Thanks to the interactions between signal and pump dictated by cross-polarization modulation (XpolM, i.e., the polarization-sensitive part of the Kerr effect), the signal SOP at the fiber output is attracted toward that of the controlling pump, regardless of the signal SOP at the fiber input, provided that the nonlinear fiber is randomly birefringent [13]. Specifically, since the nonlinear propagation through a randomly birefringent fiber is governed by the Manakov equation [13], the attraction of the signal SOP occurs toward any pump SOP; hence, it can be controlled by merely changing the input pump SOP [13]. In the first experimental demonstration of LPA [14], instead, signal and pump, both with large power, counterpropagate in a short isotropic optical fiber. Since then, the same phenomenon has been observed and characterized in various conditions, and it has been demonstrated that it occurs also in the co-propagating configuration [15].

Exploiting LPA, we can thus design an all-optical fiber-based device to control the SOP of an optical telecom signal, by using a counter- or a co-propagating pump laser. Such a

device is called a nonlinear lossless polarizer (NLP) [12,15]; further, it does not entail any loss of signal energy due to the Kerr interaction with the controlling pump. The original counterpropagating configuration of LPA requires long (microseconds) transient times and large signal power (watts) [16]; hence, a counterpropagating NLP can repolarize only powerful signals with a slowly varying SOP. Instead, when pump and signal co-propagate, the transient time of LPA is shorter and depends on the relative propagation speed, i.e., on the pump-signal walk-off delay [15], whose value can, in turn, be optimized, for given power levels, as a function of the symbol period [17]. As a consequence, a co-propagating NLP can repolarize signals with a fast-varying SOP and can employ lower power levels.

Interesting applications of LPA have been proposed recently, including the all-optical nonlinear processing and regeneration of a 40 Gb/s modulated telecom signal [18], the design of optical flip-flop memories [19], and the enhancement of the optical signal-to-noise ratio (OSNR) of a telecom signal [20,21]. Focusing in particular upon the latter application, which we shall shortly refer to as noise cleaning, it has been shown that an all-optical *noise cleaner* device is able to almost double the OSNR of a telecom signal. Such a device can be implemented based on an NLP in one of the two configurations mentioned above. Noise cleaning based on a counterpropagating NLP [20] has proven to be effective for telecom signals whose SOP does not change across many (thousands) consecutive bits, i.e., where the *polarization coherence time* is of the order of the whole bit packet. Within such a scenario, it was demonstrated that the effectiveness of LPA is little impaired by unpolarized additive noise, at least for OSNR values

of practical interest [20]. Using an NLP in the co-propagating configuration, the noise cleaning capabilities extend to telecom signals whose polarization coherence time is as short as the bit period [21], although no direct proof was provided in [21] of the effectiveness of LPA in the presence of noise.

In this work, we aim at presenting a comprehensive picture of a noise cleaner based on NLP in both configurations. We shall compare the two solutions, with counter- and co-propagating pump, for signals with a fast or slowly varying SOP. Moreover, we shall analyze the effectiveness of co-propagating LPA with additive noise and extend to the counterpropagating configuration the method proposed in [21] to theoretically estimate the OSNR gain achieved by the noise cleaner. We shall quantify the performance of the proposed noise cleaner through the traditional notion of noise figure F and measure OSNR according to the method described by ITU-T [22] (whereas a different method was used in [20]).

2. PRINCIPLE OF OPERATION

The idea behind the noise cleaning approach is that, when a polarized signal is affected by unpolarized additive white Gaussian noise (AWGN), such as the amplified spontaneous emission (ASE) noise, one can get rid of the orthogonally polarized noise component by filtering through an ideal polarizing filter, aligned with the signal SOP. In the general case, the noiseless signal component is partially (de-)polarized. Hence, in order to obtain an OSNR enhancement, the noiseless signal should first be repolarized toward a unique SOP, coinciding with the transparent eigenstate of the polarizing filter, before passing through it. Otherwise, the polarization fluctuations of the signal would be transformed into intensity fluctuations, leading to further degradation of the OSNR. We can thus employ an NLP before the polarizing filter, whose task is to attract the signal SOP (unknown and time varying, in general) toward the transparent eigenstate of the ideal polarizing filter [20,21].

A two-stage device results, as schematically depicted in Fig. 1, where the first stage is an NLP, which is able to control the signal SOP, and the second stage is an ideal polarizing filter ($Pol.$). The three plots in Fig. 1 show how the optical power of the input signal, initially split between the horizontal (red, online) and vertical (blue, online) polarization components, is attracted by the NLP toward, e.g., the vertical polarization. This is assumed to be the transparent SOP of the $Pol.$, so that the vertically polarized optical power passes through the filter unattenuated, while the orthogonally (horizontally) polarized optical power is filtered out. A similar picture holds for any attracting SOP (hence, for any input pump SOP), provided that the attracting SOP of NLP coincides with the transparent SOP of $Pol.$, i.e., that the NLP and $Pol.$ are properly aligned. One possible method to achieve such an alignment is to rotate the orientation of $Pol.$, e.g., by using a polarization controller, so that the average power at the output of $Pol.$ is maximized. Otherwise, such an alignment could be achieved also by

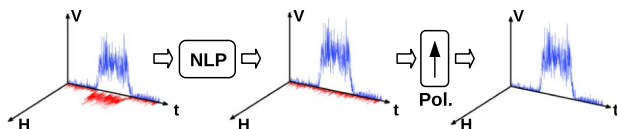


Fig. 1. Principle of operation of a noise cleaner based on a NLP.

changing the input pump SOP, while maintaining the orientation of $Pol.$ fixed. In the following, however, we will assume that the alignment between NLP and $Pol.$ is ensured, without further discussing the possible techniques to meet this condition.

If the noiseless signal component is effectively attracted by the NLP, while the unpolarized noise component is not, the resulting OSNR is enhanced. Note that signal repolarization is detrimental, if applied to polarization multiplexed formats; hence, we can apply the proposed noise cleaning strategy to optical signals with single polarization modulation formats. Consistently, in the following we shall concentrate on signals with a “legacy” binary amplitude-modulation format, i.e., on-off keying (OOK). Despite the introduction, in the last decade, of polarization multiplexed formats in high-speed (100 Gb/s) coherent optical systems, the 10 Gb/s-OOK remains the most widespread format in a nowadays optical networks scenario. Thus, although in the coming years it is expected that the 100Gb/s market will overtake the incomes of 10 Gb/s systems, in the transport networks, 10 Gb/s-OOK networks will still be used for many years, both in transport networks as well as in future metropolitan area networks. Moreover, although phase modulation formats (e.g., PSK and QPSK) with a single polarization carrier are rarely implemented, the presented device also could be employed with such formats. We conjecture that the effectiveness of the NLP could even increase, in this case, since the CW pump would interact with a signal characterized by constant intensity.

It has been shown that NLPs realized in a counterpropagating configuration or in a co-propagating configuration are characterized by different *transient times*; in all cases, they provide an effective LPA only for input signals whose SOP is stable for a period larger than their transient time [15,16]. Despite possible depolarization effects—such as polarization mode dispersion (PMD) or XPolM, suffered by the signal along the transmission channel—the *coherence time* of the noiseless signal SOP is typically much larger than that of unpolarized noise. Hence, an NLP can be designed so as to effectively act only on the noiseless signal component and not on the noise. The proposed device thus exploits a novel approach, to discriminate noise power from signal power, based on polarization rather than on frequency, as is typical of optical bandpass filters (OBPF), which are present at the front end of an optical receiver. A fundamental difference between the two approaches is that the noise cleaner is able to mitigate not only the noise power outside the signal bandwidth, but also that within the signal bandwidth, while preserving the signal power.

Assuming an ideal behavior of the NLP, the SOP of the noiseless input signal component would be attracted toward the transparent eigenstate of $Pol.$ and pass through it without any power loss, while unpolarized noise would not be attracted and remain unpolarized, so that half of its power would be suppressed by $Pol.$ We are thus tempted to conclude that the noise cleaner can increase the OSNR by 3 dB, which is then the theoretical maximum OSNR gain achievable by the device in Fig. 1. This is, however, the application of a linear reasoning to a nonlinear device, where the superposition of effects does not hold; hence, the noise cleaner performance has to be directly verified. In the following, we numerically evaluate the noise cleaner performance, as obtained in different scenarios.

3. SYSTEM SETUP AND SIMULATION PARAMETERS

Figure 2(a) shows the proposed noise cleaner setup, which we numerically simulated. The first section is an NLP, where a fully polarized CW pump laser, with power P_p , is coupled with the input signal, so as to attract the signal SOP toward the pump SOP. The NLP can be realized in the counterpropagating configuration [12–14,20], as detailed in Fig. 2(b), where signal-pump coupling is accomplished by two optical circulators. Otherwise, one can employ an NLP in the co-propagating configuration [15,17,21], as in Fig. 2(c), where signal and pump are first coupled, then the signal is isolated by the OBPF, after propagation. In both cases, the NLP includes a $L = 20$ km long dispersion-shifted fiber (DSF), with attenuation $\alpha = 0.2$ dB/km and Kerr coefficient $\gamma = 1.99$ W⁻¹ km⁻¹. The fiber is randomly birefringent, with a PMD coefficient $D_{\text{PMD}} = 0.05$ ps/km^{0.5} (a typical value for low PMD fibers), so that propagation is governed by the Manakov equation, and LPA occurs toward any pump SOP [13,16].

As recalled in Section 2, the two NLP configurations are characterized by different transient times and, hence, are suitable for input signals with different polarization coherence times. We numerically simulated the noise cleaner in Fig. 2 by injecting input signals with different polarization coherence times, power, and duration. In all cases, the input signal was placed at the fiber zero dispersion wavelength (λ_{zdw}) and is represented by the (low-pass equivalent) Jones vector $E_{tx}(t) = A_{tx}(t) + W(t)$, where the noiseless input $A_{tx}(t)$ is an intensity-modulated telecom signal with a fixed mean power P_s , while $W(t)$ is unpolarized AWGN, modeling ASE noise, whose power P_w is varied so as to test different values of $\text{OSNR}_{\text{in}} = P_s/P_w$. For the practical values of OSNR_{in} tested here (larger than 10 dB), the amount of nonlinear distortion is effectively dictated by signal power and not by noise power.

The signal output by the NLP is $E_{rx}(t) = A_{rx}(t) + N(t)$, where noise $N(t)$ is no longer white. As further discussed in Section 5, colored noise makes the measurement of the output OSNR sensitive to the bandwidth of the signal spectrum, which is broadened by Kerr distortions, during nonlinear

propagation. While XpolM is the driving force of LPA, self- and cross-phase modulations (SPM, XPM) are irrelevant for LPA. Being the pump CW, XPM just yields a constant phase shift, while SPM produces a spectral broadening of the signal. The last Kerr distortion is degenerate four-wave mixing (FWM), which is negligible, for the parameter values used here, as we numerically verified. The purpose of the “SPM Comp.” subsystem in Fig. 2(d) is to remove the SPM-induced spectral broadening, in order to ease OSNR measurement. The task of equalizing SPM distortions, which is normally unfeasible in the analog domain, can be accomplished here by a phase modulator driven by the photodetected (PD) signal intensity [23], since chromatic dispersion is absent at the signal wavelength λ_{zdw} .

The output OSNR was measured before ($\text{OSNR}_{\text{out}}^{\text{pre}}$) and after ($\text{OSNR}_{\text{out}}^{\text{post}}$) the polarizing filter $Pol.$, as shown by the blocks in Fig. 2(a). In all simulations, we ensured that, as remarked in Section 2, the pump SOP and the transparent eigenstate of $Pol.$ are aligned with each other, so that only the attracted portion of signal (and noise) passes through the filter and contributes to the measurement of $\text{OSNR}_{\text{out}}^{\text{post}}$.

4. POLARIZATION CONTROL OF A NOISY SIGNAL

Unpolarized noise degrades the degree of polarization (DOP) of the input signal; hence, it can spoil the mutual time coherence of pump and signal SOPs, which is, as stated, a necessary prerequisite for LPA. Although the performance of NLPs has been characterized as a function of system parameters [11–13,16], few studies account for the presence of noise in the attracted signal [18,20,21]. Specifically, the effectiveness of an NLP for a noisy signal, verified in [20] for the counterpropagating NLP, had never been verified in the co-propagating configuration, until recently [24]. Thus, we analyzed the performance of an NLP, in the presence of noise, in both counter- and co-propagating configurations, for input signals characterized by a polarization coherence time that is either “long,” i.e., of the order of a bit packet (*packetwise polarized signals*), or “short,” i.e., of the order of a single bit (*bitwise*

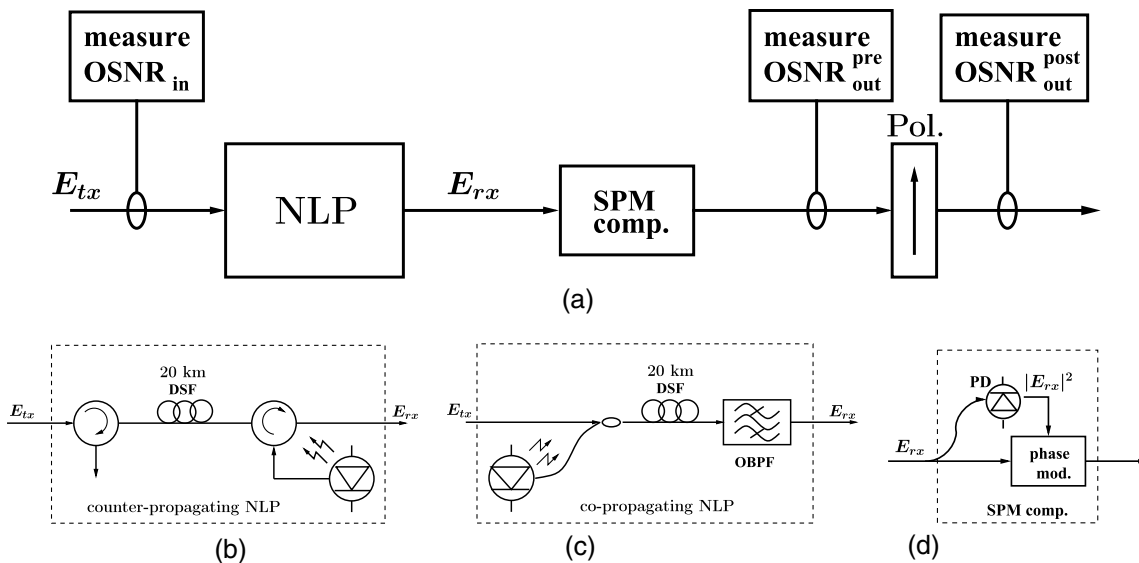


Fig. 2. (a) Noise cleaner setup, with detail of NLP architecture in the (b) counterpropagating or (c) co-propagating configuration. (d) Schematic of the SPM compensating subsystem.

polarized signals). Hence, referring to a “legacy” bit rate of 10 Gb/s, the polarization coherence time ranges between 100 ps (a single bit period) and about 1 μ s (a long Ethernet packet of 10^4 bits).

To quantify the performance of an NLP in the case of completely polarized input signals, one can evaluate the degree of attraction (DOA) [12], which is a normalized measure ($\in [-1; 1]$) of how much the signal SOP is attracted onto the input pump SOP:

$$\text{DOA} = \frac{\langle \vec{s}_s(t) \rangle}{\langle s_{0s}(t) \rangle} \cdot \hat{s}_p. \quad (1)$$

In Eq. (1), $\vec{s}_s(t)$ is the signal Stokes vector, whose amplitude is $s_{0s}(t)$, \hat{s}_p is the unit magnitude Stokes vector representing the (time invariant) pump SOP, angular brackets denote time averaging, and the dot denotes inner product. The maximum theoretical value, $\text{DOA} = 1$, is obtainable only in the case of a signal whose (constant) SOP is aligned with the attracting pump SOP. Otherwise, $\text{DOA} = 1$ represents an asymptotic value for all partially polarized signals. When the input signal SOP varies, as in all practical cases, no matter how large the coherence time is, one must perform an ensemble averaging of the output DOA values, over all possible input SOPs, i.e., calculate [12]

$$\overline{\text{DOA}} = \frac{E[\langle \vec{s}_s(t) \rangle]}{\langle s_{0s}(t) \rangle} \cdot \hat{s}_p, \quad (2)$$

where $E[\cdot]$ represents statistical averaging. It can be shown [15] that, at least in the case of fibers with moderate PMD, such an averaging yields the same result as the evaluation of the output DOP ($\overline{\text{DOA}} = \text{DOP}$), which is defined as

$$\text{DOP} = \frac{\|E[\langle \vec{s}_s(t) \rangle]\|}{\langle s_{0s}(t) \rangle}, \quad (3)$$

where $\|\cdot\|$ represents the Euclidean norm. Since the nonlinear fiber employed in this work and described in Section 3 has the same PMD coefficient as that analyzed in [15], we can quantify the performance of the NLP through the DOP of the output signal, for any polarization coherence time.

A. Packetwise Polarized Signals (Slowly Varying SOP)

We first analyze the NLP effectiveness in controlling the SOP of an amplitude-modulated optical signal characterized by a “slowly varying” SOP, i.e., of a packetwise polarized signal, whose polarization is constant over the entire packet. For these signals, an NLP designed in the counterpropagating configuration [Fig. 2(b)] has already been proven to be effective in controlling the signal SOP in a noiseless scenario [13,16].

As demonstrated in [12], the repolarization obtained by a counterpropagating NLP on an intensity-modulated, fully polarized bit packet, with mean power P_s , is the same as that obtained on an input signal consisting of a single polarized pulse, with the same energy and power P_s . We set the pulse duration to $T_s = 1$ μ s, so that it is representative of a packet of 10^4 OOK bits (@10 Gb/s) [12]. We set the pump SOP as linear horizontal (the same results are obtained for any other pump SOP, as verified [13]), to which the polarizing filter *Pol.* in Fig. 2(a) is aligned, while the input signal SOP is varied for

each transmitted packet, so that, statistically, it uniformly covers the Poincaré sphere.

To avoid packet-to-packet nonlinear interactions mediated by the pump, we assume, for the moment, that only one packet travels into the NLP at a time, so that it interacts with a “fresh” pump portion, which had not interacted with any other packet before.

In order to obtain an effective attraction of the noiseless signal, with a counterpropagating NLP, powerful signals are needed [12–14]. Exploiting a property of LPA, whose performance roughly depends on the product between signal and pump power [12], we employed strongly unbalanced power levels. In order to limit SPM, we set the signal mean power to $P_s = 0.6$ W, much less than the pump power $P_p = 2.4$ W.

Simulation results, reported in Fig. 3, show that a significant $\text{DOP} \cong 0.8$ is reached, at the output of the NLP, for a noiseless input signal, plotted as a reference, with a dotted-dashed line. The (superimposed) solid line with symbols represents the DOP obtained for a noisy input signal, as a function of OSNR_{in} , in a range of practical interest. Results clearly show that the control of the signal SOP performed by the NLP is not spoiled by the presence of additive noise; hence, an effective performance of the noise cleaner can be expected, at least for the OSNR_{in} values tested here. A further decrease of the OSNR_{in} , below 15 dB, would result in a gradual DOP degradation, due to the addition of unpolarized noise, as demonstrated in [20]. For each DOP value in Fig. 3, simulation results were averaged over 100 random input packet SOPs and 10 random noise realizations. Counterpropagation of signal and pump was numerically solved using the SCAOS algorithm [13].

As already stated, the effectiveness of the counterpropagating NLP does not extend to signals with polarization coherence times much shorter than a microsecond because of the longer transient time of the LPA process [16]. A degradation of the NLP performance for shorter signals can be observed in Fig. 4, reporting the DOP obtained at the NLP output, for noiseless packetwise polarized signals whose duration ranges from $T_s = 250$ ns to $T_s = 1.25$ μ s, i.e., packets with typical size for a packet-switched optical network operating at @10 Gb/s. In particular, the solid black line with circles, obtained by injecting isolated packets into the NLP, shows how the DOP rapidly decreases with the packet size,

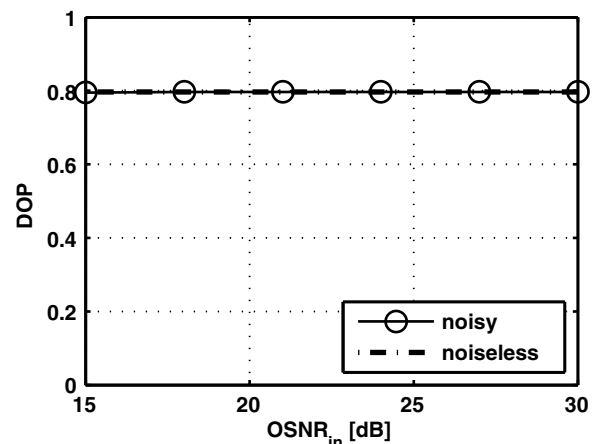


Fig. 3. Performance of a counterpropagating NLP, obtained for packetwise polarized signals.

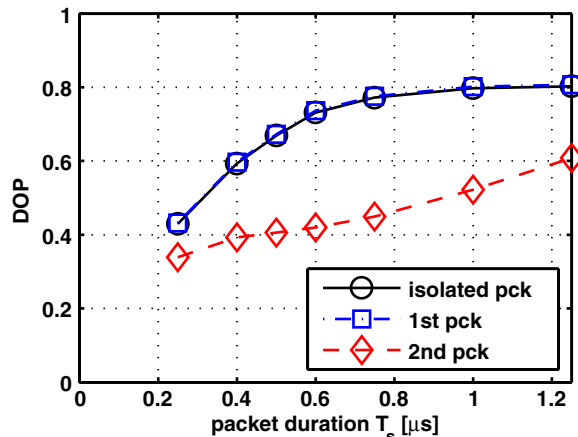


Fig. 4. Performance of a counterpropagating NLP, obtained for packetwise polarized signals with different durations. Different curves are obtained by injecting into the NLP isolated packets (solid with circles) or two consecutive packets (dotted-dashed with squares and dashed with diamonds).

due to a signal duration shorter than the NLP transient time, while, for longer packets, the output DOP seems to saturate around $\text{DOP} \cong 0.8$, confirming that the transient time of a counterpropagating NLP is about $1 \mu\text{s}$, which is in agreement with [16].

Isolated packets always interact with an undistorted pump, while in a realistic scenario packets propagate in sequence through the NLP. The dotted-dashed blue line with squares and the red dashed line with diamonds, in Fig. 4, show the DOP obtained at the NLP output by injecting two consecutive (polarized) packets, with the same duration but with independent polarization. The DOP obtained for the first packet (dot-dashed blue line) exactly coincides with that obtained for isolated packets (solid black line). This occurs because, thanks to the counterpropagating geometry of the NLP, the first packet interacts with the pump in the same way as for an isolated packet. This is no longer true for the following packet (dashed red line), whose DOP degrades significantly. This is due to its interaction with a pump portion that was previously distorted by the nonlinear polarization rotation occurred with the preceding packet. Hence, the pump SOP is changed, with respect to its input SOP, and so are the polarization interactions between the pump and the second packet. Despite the moderate increase of DOP versus packet duration, the polarization attraction of the second packet (dashed line in Fig. 4) is impaired and, if a third packet propagated in sequence through the NLP, its resulting output DOP would be further degraded, as we numerically verified.

It is thus clear that packet-to-packet nonlinear interactions mediated by the pump are detrimental for the NLP operation. Indeed, within LPA, the pump represents a resource that “is consumed” by the signal packets. To guarantee a “refreshing” of the consumed pump, and to avoid the consequent performance degradations, a guard interval is needed, between two consecutive packets injected into the NLP, enabling the distorted portion of the pump to exit the NLP. In the results that follow in Section 5, when analyzing the noise cleaner operation with a counterpropagating NLP, we will assume that such a guard interval between two consecutive packets is guaranteed (e.g., by a sufficiently low traffic load of the optical network).

B. Bitwise Polarized Signals (Fast-Varying SOP)

Given the severe performance degradation of a counterpropagating NLP in controlling the SOP of a short packet, i.e., of an input signal whose duration is shorter than the transient time of the NLP, we cannot expect any gain on the OSNR of such signals, from the noise cleaner with NLP realized as in Fig. 2(b). A solution is to implement the NLP in the co-propagating geometry, shown in Fig. 2(c), which has been proven able to control the SOP of signals with duration as short as the bit period [15]. In order to verify its potentials, we evaluated its performance for modulated bit packets whose polarization coherence time is of the order of one bit period; hence, for bitwise polarized signals. In numerical simulations, the transmitted noiseless signal $A_{tx}(t)$ consisted of a stream of 2560 bits with OOK modulation at 10 Gb/s ($T_s = 256 \text{ ns}$), with a random SOP of each OOK pulse, uniformly distributed over the Poincaré sphere, so that the input DOP is zero.

In Section 4.A, we have seen how packet-to-packet nonlinear interactions mediated by the pump are detrimental for the repolarization of consecutive packets. Similarly, for bitwise polarized signals, the bit-to-bit nonlinear interactions mediated by the pump are detrimental for the co-propagating NLP performance, and we should avoid them. To do so, we chose a return-to-zero (RZ-OOK) modulation format, so as to introduce a guard interval between two consecutive OOK pulses. Moreover, as demonstrated in [17], the effectiveness of a co-propagating NLP is maximized when the walk-off delay between signal and pump is roughly twice the signal pulse duration. In order to satisfy both conditions above, we chose a RZ-OOK format with duty-cycle 33%. Hence, in the simulation results that follow, each bit is encoded on a pulse with duration $T_p = 33.3 \text{ ps}$, and a nearly optimal walk-off $T_D = 64 \text{ ps}$ can be reached by properly placing the pump wavelength, as in [17,21]. Furthermore, $T_p + T_D$ is less than the bit period ($T_b = 100 \text{ ps}$), which guarantees the absence of nonlinear pulse-to-pulse interactions mediated by the pump.

Figure 5 shows the DOP of the output noisy signal $E_{rx}(t)$ as a function of OSNR_{in} (solid line with symbols). Results were obtained by setting the pump power at $P_p = 0.4 \text{ W}$ and the signal mean power at $P_s = 33.3 \text{ mW}$ (peak power equal to 200 mW). The overall transmitted power is almost an order of magnitude lower than the one transmitted in Section 4.A, which demonstrates the superior power efficiency of the co-propagating NLP configuration [20,21]. The DOP obtained for a noiseless input signal, equal to 0.86, is plotted along as a reference (dotted-dashed line). For lower OSNR_{in} values, the decrease of the output DOP demonstrates a degradation of the NLP effectiveness. As was already observed for a counterpropagating NLP [20], part of the decrease of DOP is a trivial consequence of the addition of unpolarized noise at the input. Nonetheless, comparing results in Figs. 3 and 5 proves that a co-propagating NLP, with input signals characterized by a fast-varying SOP, is more sensitive to noise than a counterpropagating NLP.

It should be remarked that the effectiveness of the co-propagating NLP, just shown for bitwise polarized signals, also extends to signals with longer polarization coherence times, such as those examined in Section 4.A. For the same system parameters used in Fig. 5, we obtained the same DOP values, when increasing the coherence time of the transmitted

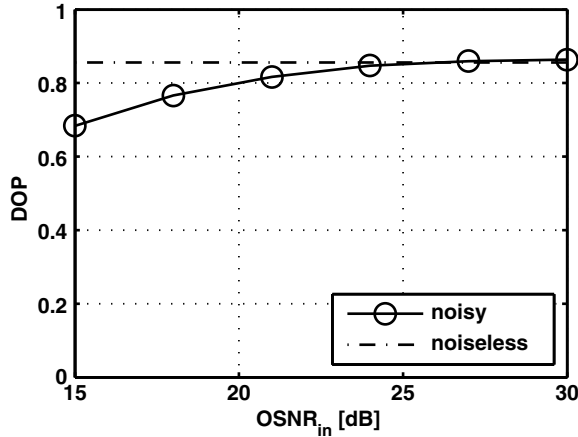
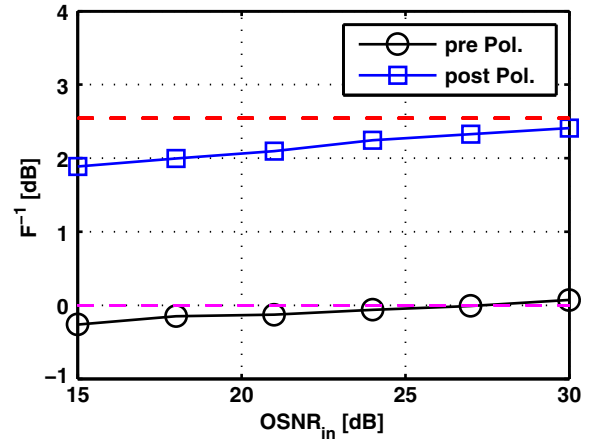


Fig. 5. Performance of an optimized co-propagating NLP, obtained for bitwise polarized signals (as well as for longer polarization coherence times).

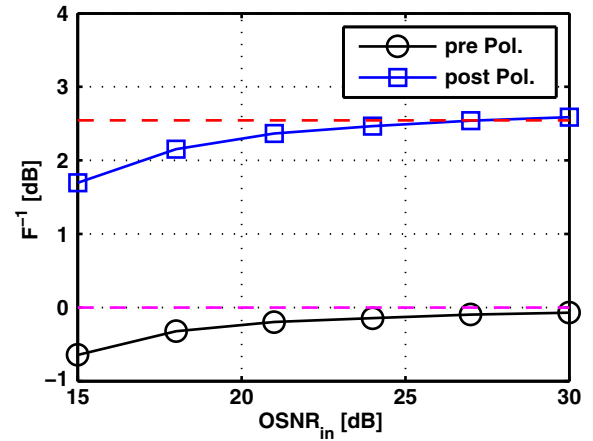
signal. Such a flexibility of the co-propagating NLP configuration occurs here because the key system parameters (i.e., the duty cycle of the signal and the total walk-off delay between signal and pump) were selected ad hoc, so that each pulse interacts with the pump as if it were propagating alone into the NLP, no matter how many consecutive pulses are transmitted. With the parameters chosen here, it is as if each pulse had a dedicated portion of the pump, with the duration of one bit period T_b , to perform LPA toward the pump SOP. This is no longer true when the duty cycle of the RZ-OOK modulation increases, since the conditions for the simultaneous achievement of an optimal walk-off ($T_D \simeq 2T_p$) and a proper guard interval between adjacent pulses ($T_b - T_p \geq T_D$) cannot be satisfied. The limiting case is that of a 100% duty cycle, i.e., to a NRZ-OOK modulated signal: since there is no guard interval between adjacent pulses, the walk-off delay should be zero; hence, signal and pump should propagate at the same speed, within the NLP. Under this condition, the co-propagating NLP works in the *polarization rotation regime* [17], where signal and pump SOPs evolve along circles, on the Poincaré sphere, as opposed to the *polarization attraction regime* where, due to the mutual sliding between pump and signal given by the walk-off, the signal SOP follows a spiral trajectory that collapses onto the input pump SOP [17]. Co-propagating NLPs operating in the polarization rotation regime have already been shown to have poor repolarization performance [25], compared with those operating in the polarization attraction regime, i.e., with a proper walk-off [15]. Hence, if an NRZ signal is to be attracted (that is, packetwise polarized and long enough), the counterpropagating NLP, analyzed in Section 4.A, remains the most effective solution.

5. NOISE CLEANING

After the NLP stage has performed an LPA of the signal toward the pump SOP, the *Pol.* stage yields an OSNR gain by filtering out the noisy signal component orthogonal to it. In order to estimate the OSNR gain, we resorted to the classical definition of noise figure, $F = \text{OSNR}_{\text{in}}/\text{OSNR}_{\text{out}}$, and calculated F^{-1} , both before and after the polarizing filter *Pol.*, as depicted in Fig. 2(a):



(a)



(b)

Fig. 6. Inverse noise figure F^{-1} , evaluated before (pre) and after (post) the polarizing filter, which yields the OSNR gain. Simulation results are obtained for a noise cleaner with a (a) counter- or a (b) co-propagating NLP configuration.

$$F_{\text{pre,post}}^{-1} = \frac{\text{OSNR}_{\text{out}}^{\text{pre,post}}}{\text{OSNR}_{\text{in}}}. \quad (4)$$

All OSNR values were numerically evaluated according to ITU-T recommendations [22], on a standard reference bandwidth $B_0 = 0.1$ nm. In particular, the noisy signal was first filtered on the signal bandwidth, to get the signal plus noise power $P_T = P_R + P_N$, then on an outer noise bandwidth, to estimate noise power P_N alone. The output OSNR was eventually evaluated as $\text{OSNR} = (P_T - P_N)/P_N$. Note that the noise power measured on the two bandwidths is the same ($P_N = P'_N$) if and only if the output noise is white. Since the NLP is a nonlinear device, one must expect a colored noise at the output and, accordingly, some mismatches in the measurements.

Figure 6 shows F^{-1} as a function of OSNR_{in} , which is obtained for a noise cleaner with a counter- (a) or a co-propagating (b) NLP configuration. In the first case [Fig. 6(a)], the input signal is the (isolated) packetwise polarized signal with $T_s = 1 \mu\text{s}$ (i.e., that used to obtain Fig. 3); otherwise, the counterpropagating noise cleaner is not effective (as was numerically verified in Fig. 4). In the second case [Fig. 6(b)], the input signal is the bitwise polarized signal with RZ-OOK

33% (i.e., that used to obtain Fig. 5), although the co-propagating noise cleaner is equally effective for signals with slowly varying SOP (as was numerically verified), as a consequence of an equally effective repolarization, which is verified in Section 4.B. In both Figs. 6(a) and 6(b), the solid line with circles (black) and that with squares (blue), report the F^{-1} values obtained by measuring OSNR_{out} before or after the Pol. , respectively, as evidenced in Fig. 2(a) by the blocks labeled “measure $\text{OSNR}_{\text{out}}^{\text{pre,post}}$ ”.

The top dashed lines (red) represent an upper limit to the performance of the device and are located at 2.5 and 2.7 dB, in Figs. 6(a) and 6(b), respectively. As further discussed in Section 6, such a limit is due to the nonideal polarization control performed by the NLP on the signal, as evidenced by the DOP values in Figs. 3 and 5. Even in the noiseless case, a $\text{DOP} < 1$ reveals that a portion of the output signal power is still orthogonal to the pump polarization; hence, it is suppressed by the Pol. , along with half the noise power. If the ideal condition $\text{DOP} = 1$ were met by the NLP, the upper limit for the noise cleaner performance would be 3 dB.

On the other hand, the lower dashed (magenta, online) lines in Figs. 6, located at 0 dB, represent the theoretical reference value that should be measured before the polarizing filter Pol. . In fact, the measurement of $\text{OSNR}_{\text{out}}^{\text{pre}}$ should yield exactly the same value as OSNR_{in} , since, as seen in Fig. 2, the noisy input field $E_{\text{tx}}(t)$ undergoes pure phase and polarization distortions, both in the fiber (SPM, XPM, XpolM) and in the phase modulator, up to Pol. . Thus, there is no exchange of energy between the frequency components of signal and noise; hence, their power ratio (unaffected by scattering loss) is constant. However, as lower OSNR_{in} values were tested by increasing the “noise load” P_w , the total transmitted power increases and so does the spectral broadening of the signal (despite SPM compensation). A consequent “leakage” of signal power onto the noise measurement bandwidth yields an overestimation of P_N , at the expense of an underestimated P_T , as we numerically verified, causing an increasing underestimation of OSNR_{out} .

Indeed, the artifact described above, which causes the mismatch between simulation results for F_{pre}^{-1} and its theoretical zero value in Fig. 6, is related to the standard OSNR measurement technique [22]; hence, it affects both solid curves of each plot in Fig. 6. Thus, to get rid of such an artifact, we can estimate the actual OSNR gain G as the difference (in dB) between the solid curves in Fig. 6, i.e.,

$$G = \frac{F_{\text{post}}^{-1}}{F_{\text{pre}}^{-1}} = \frac{\text{OSNR}_{\text{out}}^{\text{post}}}{\text{OSNR}_{\text{out}}^{\text{pre}}}. \quad (5)$$

Figure 7 shows G , plotted with solid (black) lines, which is obtained by a noise cleaner realized with a counter- or a co-propagating NLP configuration [Figs. 7(a) and 7(b), respectively]. In both cases, we obtained an OSNR gain between 2 and 3 dB, demonstrating that the proposed noise cleaner can effectively regenerate amplitude-modulated optical signals. As mentioned in Section 2, exploiting the polarization to discriminate noise power from signal power, the noise cleaner is able to mitigate noise power even within the signal bandwidth, while preserving the signal power.

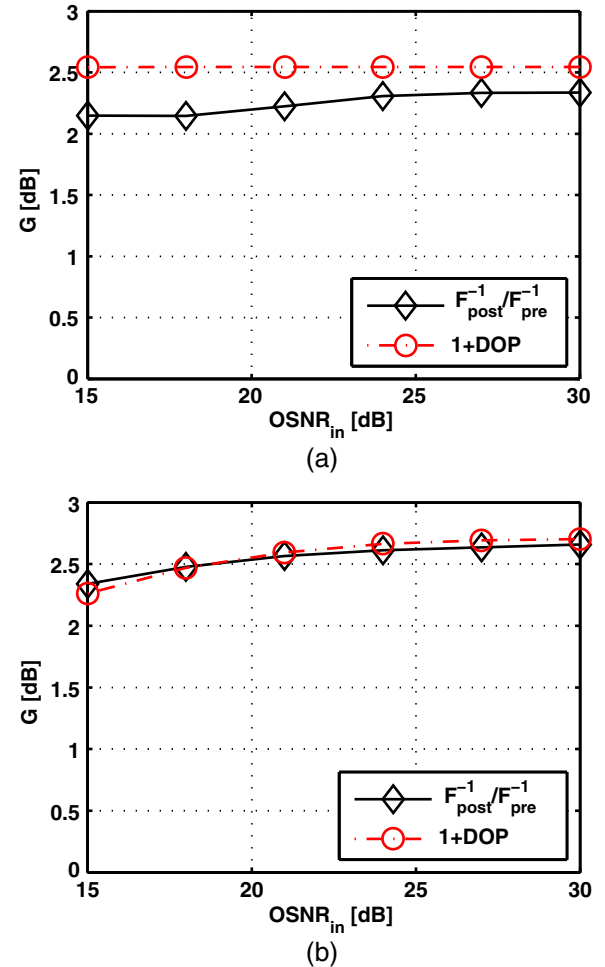


Fig. 7. Effective OSNR gain, calculated as the increase in the inverse noise figure F^{-1} , due to a noise cleaner with a counter- (a) or a co-propagating (b) NLP configuration. Dashed lines show the results of the theoretical approximation, as a function of input OSNR: $G = 1 + \text{DOP}$.

6. THEORETICAL APPROXIMATION

The dashed red curves in Fig. 7 represent an estimate of G , which can be evaluated from the measurement of the DOP of the signal output by the NLP, as follows.

In addition to the DOP, the effectiveness of an NLP, in the absence of noise, can be quantified by the average fraction ρ of signal power that has the same SOP as the pump [12,14]. Being the pump SOP aligned with the polarizing filter Pol. , ρ is the fraction of signal energy that passes through Pol. in Fig. 2(a). As opposed to a noiseless signal, pure input noise is not attracted and remains unpolarized at the output, as numerically verified, so that 50% of its power is suppressed by Pol. . Although linearity does not hold here, we can approximate G as the ratio of attracted signal-to-noise power: $\rho/0.5$. In the absence of noise ($\text{OSNR}_{\text{in}} = \infty$), simulation results showed that ρ equals 0.90 for the counterpropagating NLP acting on a packetwise-polarized signal (Section 4.A), while $\rho = 0.93$ results for the co-propagating NLP acting on a bitwise-polarized signal (Section 4.B). Hence, 90% or 93% of the signal power was attracted toward the pump SOP in the two scenarios. From these figures, we obtained the approximate G , which is equal to $0.90/0.5$ (2.5 dB) and $0.93/0.5$ (2.7 dB),

respectively, marked by the upper dashed red lines in Fig. 6. Further theoretical analysis of LPA in the noiseless case [12] has shown that the fraction ρ is, in turn, related to the DOP of the output signal $E_{rx}(t)$ by the simple relationship $\rho = (1 + \text{DOP})/2$, where DOP is obviously evaluated before the *Pol.* (one would trivially get $\text{DOP} = 1$, after the polarizing filter). This relationship is not surprising, since DOP quantifies the alignment between the average signal SOP and the pump SOP [15]. Still assuming that the output unpolarized noise power is halved by *Pol.*, the approximation derived above for G becomes $\rho/0.5 = (1 + \text{DOP})$, as reported in Fig. 7, with red dashed lines. Note that the OSNR gain estimates in Figs. 7(a) and 7(b) as a function of OSNR_{in} were evaluated straightforwardly, i.e., by summing 1 to the numerical values in Figs. 3 and 5 (and converting to the log scale).

As seen in Fig. 7, DOP decreases with OSNR_{in} , as the input noise increases. As stated in Section 4.B, the degradation of the output DOP is an expected behavior, which is physically related to the decrease of the input DOP due to the additive noise, despite the repolarization provided by the NLP. In Fig. 7, we can see a very good match between the theoretical approximation and the actual OSNR gain reached by the noise cleaner, at least in the co-propagating configuration. Larger discrepancies are observed in Fig. 7(a), for the counterpropagating configuration. The difference between G and its estimate is, however, below 0.4 dB, compared with OSNR gain values always above 2 dB, in any of the tested configurations, further confirming the noise cleaning capabilities of the proposed device.

7. CONCLUSION

We proposed a novel all-optical noise cleaning device, conceived for modulated optical signals with a single polarization carrier. The noise cleaner is based on the simple concept of suppressing the orthogonally polarized half of additive noise through a polarizing filter, hence ideally reaching a 3 dB enhancement of the OSNR. The discrimination of noise power from signal power relies on the SOP; hence, the device is able to mitigate even noise power lying within the signal bandwidth, while fully preserving signal power. The core of the device is a NLP, which is able to dynamically control the time-varying SOP of partially polarized signals. Recent studies on LPA have shown that the NLP can be realized in two different configurations, with a counter- or a co-propagating pump laser. In this work, we tested, by numerical simulations, both configurations of the device and applied them to the noise cleaning of signals with amplitude modulation at 10 Gb/s and with different speeds of variation of their polarization (i.e., different *polarization coherence time*).

Results show that signals with a polarization that is constant over thousands of bits (i.e., for *packetwise-polarized signals*) benefit by both configurations of the noise cleaner, with an effective gain of the OSNR between 2 and 3 dB, at least for the tested input OSNR of practical interest. A similar gain was obtained as well for signals with a fast-varying polarization, on the scale of a bit period (i.e., for *bitwise-polarized signals*), by resorting to the co-propagating configuration of the noise cleaner. Thus, we showed that the more recently devised (and less studied) co-propagating LPA is more flexible and more power efficient, with a reduction of the overall average transmitted power from 3 W to less than 0.5 W. We

showed that the achieved OSNR gain is strictly related to the performance of the NLP and can be theoretically estimated after measuring the DOP of signals at its output.

REFERENCES

1. M. Martinelli, P. Martelli, and S. M. Pietralunga, "Polarization stabilization in optical communications systems," *IEEE J. Lightw. Technol.* **24**, 4172–4183 (2006).
2. S. Popov and E. Vanin, "Polarization dependence of Raman gain on propagation direction of pump and probe signal in optical fibers," in *Proceedings of Laser and Electro-Optics (CLEO)*, (IEEE, 2001), paper CTuJ5.
3. S. Popov, S. Sergeev, and A. T. Friberg, "The impact of pump polarization on the polarization dependence of the Raman gain due to the breaking of a fiber's circular symmetry," *J. Opt. A Pure Appl. Opt.* **6**, S72–S76 (2004).
4. M. Martinelli, M. Cirigliano, M. Ferrario, L. Marazzi, and P. Martelli, "Evidence of Raman-induced polarization pulling," *Opt. Express* **17**, 947–955 (2009).
5. L. Ursini, M. Santagiustina, and L. Palmieri, "Raman nonlinear polarization pulling in the pump depleted regime in randomly birefringent fibers," *IEEE Photon. Technol. Lett.* **23**, 254–256 (2011).
6. S. V. Sergeev, "Activated polarization pulling and decorrelation of signal and pump states of polarization in a fiber Raman amplifier," *Opt. Express* **19**, 24268–24279 (2011).
7. S. Sergeev and S. Popov, "Two-section fiber optic Raman polarizer," *IEEE J. Quantum Electron.* **48**, 56–60 (2012).
8. N. J. Muga, M. F. S. Ferreira, and A. N. Pinto, "Broadband polarization pulling using Raman amplification," *Opt. Express* **19**, 18707–18712 (2011).
9. A. Zadok, E. Zilka, A. Eyal, L. Thévenaz, and M. Tur, "Vector analysis of stimulated Brillouin scattering amplification in standard single-mode fibers," *Opt. Express* **16**, 21692–21707 (2008).
10. J. E. Heebner, R. S. Bennink, R. W. Boyd, and R. A. Fisher, "Conversion of unpolarized light to polarized light with greater than 50% efficiency by photorefractive two-beam coupling," *Opt. Lett.* **25**, 257–259 (2000).
11. M. Barozzi and A. Vannucci, "Performance analysis of lossless polarization attractors," in *Latin America Optics and Photonics Conference*, OSA Technical Digest (online) (Optical Society of America, 2012), paper LM3C.4.
12. M. Barozzi and A. Vannucci, "Performance characterization and guidelines for the design of a counter-propagating nonlinear lossless polarizer," *J. Opt. Soc. Am. B* **30**, 3102–3112 (2013).
13. M. Barozzi, A. Vannucci, and D. Sperti, "Lossless polarization attraction simulation with a novel and simple counterpropagation algorithm for optical signals," *J. Eur. Opt. Soc. Rapid Pub.* **7**, 12042 (2012).
14. S. Pitois, J. Fatome, and G. Millot, "Polarization attraction using counterpropagating waves in optical fiber at telecommunication wavelengths," *Opt. Express* **16**, 6646–6651 (2008).
15. V. V. Kozlov, M. Barozzi, A. Vannucci, and S. Wabnitz, "Lossless polarization attraction of copropagating beams in telecom fibers," *J. Opt. Soc. Am. B* **30**, 530–540 (2013).
16. V. V. Kozlov, J. Fatome, P. Morin, S. Pitois, G. Millot, and S. Wabnitz, "Nonlinear repolarization dynamics in optical fibers: transient polarization attraction," *J. Opt. Soc. Am. B* **28**, 1782–1791 (2011).
17. M. Barozzi and A. Vannucci, "Optimal pump wavelength placement in lossless polarization attraction," in *Proceedings of Fotonica 2013* (AEIT—Federazione Italiana di Elettrotecnica, Eletttronica, Automazione, Informatica e Telecomunicazioni, 2013), paper P.12.
18. P. Morin, J. Fatome, C. Finot, S. Pitois, R. Claveau, and G. Millot, "All-optical nonlinear processing of both polarization state and intensity profile for 40 Gbit/s regeneration applications," *Opt. Express* **19**, 17158–17166 (2011).
19. P.-Y. Bony, M. Guasoni, E. Assémat, S. Pitois, D. Sugny, A. Picozzi, H. R. Jauslin, and J. Fatome, "Optical flip-flop memory and data packet switching operation based on polarization

- bistability in a telecommunication optical fiber," *J. Opt. Soc. Am. B* **30**, 2318–2325 (2013).
20. M. Barozzi and A. Vannucci, "A novel device to enhance the OSNR based on lossless polarization attraction," in *Proceedings of Fotonica 2013* (AEIT—Federazione Italiana di Elettrotecnica, Elettronica, Automazione, Informatica e Telecomunicazioni, 2013), paper C6.5.
 21. M. Barozzi and A. Vannucci, "All-optical noise cleaning based on co-propagating lossless polarization attraction," in *Proceedings of IEEE International Conference on Photonics (ICP 2013)*, doc. ID 1569795661 (IEEE, 2013), paper D3-AM1-C.2.
 22. "Optical system design and engineering considerations," ITU-T Series G Supplement 39 (09/2012).
 23. C. Xu, L. Mollenauer, and L. Xiang, "Compensation of nonlinear self-phase modulation with phase modulator," *Electron. Lett.* **38**, 1578–1579 (2002).
 24. M. Barozzi, A. Vannucci, and G. Picchi, "All-optical polarization control and noise cleaning based on a nonlinear lossless polarizer," *Proc. SPIE*, doc. ID PPR100-71 (to be published).
 25. V. V. Kozlov, K. Turitsyn, and S. Wabnitz, "Nonlinear repolarization in optical fibers: polarization attraction with copropagating beams," *Opt. Lett.* **36**, 4050–4052 (2011).